BBA Advances 7 (2025) 100153

Contents lists available at ScienceDirect

BBA Advances

journal homepage: www.sciencedirect.com/journal/bba-advances

Characterization of HOL-30: a novel tandem-repeat galectin from the marine sponge *Halichondria okadai*

Mayuka Ohkawa [a], Kenichi Kamata [b], Sarkar M.A. Kawsar [c], Marco Gerdol [d,*], Yuki Fujii [e,*], Yasuhiro Ozeki [a,*]

[a] Graduate School of NanoBiosciences, Yokohama City University, 22-2, Seto, Kanazawa-ku, Yokohama 236-0027, Japan
[b] Graduate School of Medical Life Science, Yokohama City University, 1-7-29, Suehiro, Tsurumi-Ku, Yokohama 230-0045 Japan
[c] Department of Chemistry, Faculty of Science, University of Chittagong, Chittagong 4331 Bangladesh
[d] Department of Life Sciences, University of Trieste, Via Licio Giorgieri 5 34127 Trieste, Italy
[e] Graduate School of Pharmaceutical Sciences, Nagasaki International University, 2825-7, Huis Tem Bosch, Sasebo 859-3298 Nagasaki, Japan

ARTICLE INFO

Keywords:
Galectin
Porifera
Halichondria okadai
Primary structure, Sponge
Transcriptome

ABSTRACT

We here report the novel primary structure of a new member in the galectin family, the β-galactoside-binding lectin HOL-30, from the marine sponge *Halichondria okadai*, whose full-length sequence was determined thanks to the combination between Edman degradation and transcriptome analysis. The HOL-30 polypeptide is a tandem-repeat dimeric galectin, consisting of 281 amino acids, which includes two carbohydrate recognition domains (CRDs). Unlike most other galectins described in Porifera, HOL-30 did not have a signal peptide sequence for secretion. In solution, HOL-30 exhibited a molecular weight of 60 kDa, indicating a dimeric organization consisting of two 30 kDa tandem-repeat subunits stabilized by non-covalent interactions. Although the two CRDs had a similar predicted 3D structure, they displayed low pairwise sequence identity, approximately 20 %. HOL-30 exhibited glycan-binding affinities for type-1 (Galβ1–3GlcNAc) and type-2 (Galβ1–4GlcNAc) LacNAc. Furthermore, it also recognized blood type B-oligosaccharides on type-1 and type-2 LacNAc (Galα1–3Gal[Fucα1–2]β1–3/4GlcNAc), and blood type H-oligosaccharide on type-3 (Gal[Fucα1–2]β1–3GalNAcα). The glycan-binding properties of HOL-30 were compared with those of the hRTL galectin, previously identified in *Chondrilla australiensis*, consisting of tetrameric 15 kDa prototype subunits. The two sponge galectins displayed similar, but not identical, carbohydrate-binding properties, as evidenced by the fact that despite effectively binding to vertebrate cultured cells, HOL-30 had minimal impact on cell growth. Antiserum analysis revealed a mosaic distribution of HOL-30 in the parenchymal cells of sponge tissues within dense cell clusters surrounding the spicules.

1. Introduction

HOL-30, a β-galactoside-binding lectin purified from the sponge *Halichondria okadai*, belonging to the phylum Porifera, subclass Heteroscleromorpha, consists of two non-covalently bound 30 kDa polypeptides. Although this protein was previously shown to belong to the galectin family [1], its moleculat characterization was limited to a partial amino acid sequence.

Galectins, one of the most representative lectin families, can be classified among three sub-types based on the structural features of their carbohydrate recognition domain (CRD). The prototype sub-type has a single CRD and functions as an oligomer. Notable examples include human galectin-1 and galectin-2, which have a 15 kDa CRD with β-sheet structures consisting of two layers: six strands form a concave surface, and five forms a convex surface. The concave surface contains a carbohydrate-binding site. The chimera sub-type, exemplified by human galectin-3, has a 15 kDa CRD at the C-terminus, accompanied by N-terminal domains that support multimerization. Finally, the tandem-repeat sub-type has two distinct CRDs arranged in tandem within the same polypeptide. These sub-types share the β-sandwich fold as the core structure of their CRD, which is the foundation of their carbohydrate-binding properties and diverse functions [2,3].

The study of the evolution and functional diversification of metazoan galectins would clearly benefit from the study of homologous sequences

* Corresponding authors.
E-mail addresses: mgerdol@units.it (M. Gerdol), yfujii@niu.ac.jp (Y. Fujii), ozeki@yokohama-cu.ac.jp (Y. Ozeki).

https://doi.org/10.1016/j.bbadva.2025.100153
Received 25 October 2024; Received in revised form 22 February 2025; Accepted 28 February 2025
Available online 15 March 2025

present in the other major lineages of Opisthokonta, such as Fungi and, above all, Choanoflagellata, which are recognized as the sister group of Metazoa [4]. However, without any characterized galectin from this key class of flagellate unicellular eukaryotes, Porifera emerges as a key phylum for evolutionary studies due to its basal placement in the animal tree of life. With this regard, several galectins, belonging to both the prototype [5–9,11] and tandem-repeat [10] sub-types, have been previously reported in marine sponges. The prototype galectin from the Pacific Ocean-dwelling genus *Cinachyrella*, which shares the same tetrameric structure as the prototype galectin hRTL (*Chondrilla australiensis* tetramer galectin) [6] and *C. caribensis* galectin CCL [8], currently represents the only sponge galectin whose 3-D crystal structure (PDB 4AGG) has been elucidated to date [12]. The structural comparisons between different poriferan galectins may undoubtedly provide clues for understanding the origin of the different galectin sub-types in metazoans, as well as the acquisition of a β-sandwich fold in galectins.

Compared to other galectins derived from more recent animal lineages, those of Porifera display several unique structural and functional characteristics. For example, they were shown to activate ion channels in mammalian cells [9], having synergistic effects on the inhibition of bacterial growth [5,7,8], and being highly resistant to high temperatures [6,8]. Structurally, they display low primary sequence similarity with galectins from other animal clades, such as mammals [5–11], except for the highly conserved amino acids involved in glycan-binding. Besides, different Porifera galectins are characterized by the unusual presence of N-terminal signal peptides [6,13–15]. This was first reported in the proto-type galectin CGL-1 from the Mediterranean Sea sponge *Geodia cydonium*, the first galectin ever described in this phylum [11], where cDNA cloning revealed the presence of 17 N-terminal hydrophobic amino acids that were not part of the mature protein [13]. The presence poriferan galectins undergoing signal peptide-mediated secretion was later confirmed by the analysis of the genome of the marine sponge *Amphimedon queenslandica*, a model species for studying metazoan evolution [14]. Besides identifying an N-terminal signal for canonical secretion, this genomic resource also highlighted the peculiar gene architecture of the three sponge galectin genes (LOC105313191, LOC109582911, LOC105315566). In fact, unlike the typical galectin genes of bilaterian animals, which usually show three exons, the *Amphimedon queenslandica* genes were intronless, and were intronless genes [14,15]. Another evidence supporting the widespread presence of galectins undergoing canonical secretion in sponges was provided by the finding that the six prototype galectins hRTLs from *C. australiensis* had 23 a.a. signal peptide sequences [6]. Furthermore, it is noteworthy that a few sponge galectins can recognize clinically significant glycans [6,16], suggesting that the characterization of additional galectins from Porifera may offer potential benefits for the implementation of several biotechnological applications in different domains of life science [17,18].

Here, we report the identification of the primary structure of HOL-30, along with the characterization of its glycan-binding properties, cell regulatory activities and the determination of its tissue localization. The recent functional characterization of hRTL offered us a valuable opportunity to compare the properties of these two sponge galectins, addressing a key gap in the study of lectins in this early-branching animal phylum. These findings have important implications in the field of applied glycomics, since they may allow the development of galectin-derived diagnostic or cell-regulating molecules, possibly also contributing to the development of novel glyco-drugs.

2. Materials and methods

2.1. Materials

Halichondria okadai and *Chondrilla australiensis* specimens were collected from the intertidal zone of Sagami Bay, Miura City, Kanagawa Prefecture, Japan. The human cell line HeLa (cervical cancer) was obtained from ATCC. Bovine serum albumin (BSA), Pathoprep-568, cell lysis buffer M, Mayer's hematoxylin solution, eosin alcohol solution, 4 % paraformaldehyde phosphate buffer, 20 % glutaraldehyde solution, cacodylate buffer, Canada balsam, crystal violet solution, Penicillin-Streptomycin solution, and horseradish peroxidase (HRP)-conjugated β-actin mAb were acquired from FUJIFILM Wako Pure Chemical Corp. (Osaka, Japan). Standard protein markers for SDS-PAGE were purchased from Takara Bio Inc. (Kyoto, Japan). HRP-conjugated goat anti-rabbit IgG was obtained from Tokyo Chemical Industry Co. (Tokyo, Japan). FITC-labeled goat anti-rabbit IgG was bought from Abcam (Cambridge, UK). 4',6-diamidino-2-phenylindole (DAPI), RPMI 1640 medium, and fetal bovine serum (FBS) were provided by Gibco/Thermo Fisher (Waltham, MA, USA). Poly-L-lysine-coated slides were acquired from Millipore-Sigma (Darmstadt, Germany). Cell Counting Kit-8 (including WST-8[2-(2-methoxy-4-nitrophenyl)-3-(4-nitrophenyl)-5-(2,4-disulfophenyl)-2H-tetrazolium monosodium salt]), FITC Labeling kit-NH2 was secured from Dojindo Laboratories (Kumamoto, Japan). PVDF membrane for electroblotting, peroxidase substrate EzWestBlue, and Colored standard marker protein AE-1450 EzStandard PrestainBlue were purchased from ATTO Corp. (Tokyo, Japan).

2.2. Purification of lectins

HOL-30 was purified following a previously described method [1]. Two hundred grams of sponge tissues were minced with a razor and homogenized in sodium bicarbonate buffer with protease inhibitors. The homogenates were centrifuged at 14,720 × *g* for one hour at four°C, followed by another centrifugation at 27,500 × g for one hour at four°C. The supernatant was applied to a lactosyl-agarose affinity column (MiliporeSigma LLC, St. Louis, Mo USA), and the lectin was eluted using a 100 mM lactose-containing 50 mM sodium bicarbonate in saline buffer (pH 8.8). Lectin purity was analyzed by SDS-PAGE [19]. Eluted fractions were heated and loaded into a polyacrylamide gel for electrophoresis. Afterward, the gel was stained with Coomassie Brilliant Blue [20]. Protein concentrations were measured using a BCA protein assay kit (Thermo Fisher/Pierce, Waltham, MA, USA) with bovine serum albumin as the standard, and absorbance was recorded using a microplate reader (model iMark; Bio-Rad Laboratories, Hercules, CA, USA) [21,22]. The two-fold dilution method [23] measured hemagglutination activity in two dimensions. The purified lectin was vertically diluted in a V-shape bottom 96-plastic plate from A1 to H1. Then, each lectin (A-H) was again horizontally diluted from columns 1 to 12. The hemagglutination assay used 1 % (w/v) trypsinized and 0.25 % glutaraldehyde-fixed rabbit erythrocytes.

2.3. Molecular mass analysis

The purified lectins (5 μg) were subjected to SDS-PAGE and gel permeation chromatography (GPC) utilizing a Shodex KW 402.5–4F column (4.6 mm × 300 mm) connected to an HPLC pump LC-2000 and 2402 UV/VIS detector (JASCO Co., Ltd., Tokyo, Japan). HOL-30 was solved in 50 mM sodium bicarbonate in saline, and the elution time of HOL-30 from the column has monitored the absorbance at 220 nm using a detector UV-2070plus (JASCO Co., Ltd., Tokyo, Japan), detecting the peptide bond according to the vendor's instruction [6].

2.4. RNA-sequencing and primary structure analysis of HOL-30

The RNA sequencing procedure followed a previously described protocol [6]. Briefly, the *H. okadai* tissue was cut into small pieces (20 mg) using razor blades from the sponge (approximately 10 mm squares) that adhered to the rock. The sample tissue was homogenized in a vial with TRIzol (Thermo Fisher Scientific, Waltham, MA, USA). The total RNA, representing a pool of two individual sponges, was extracted following the manufacturer's instructions. Following standard quality assessment, performed with an Agilent Bioanalyzer instrument (Agilent Technologies, Santa Clara, CA, USA), and quantification, the RNA was

used as an input for the preparation of a library compatible with next-generation sequencing on a single lane of an Illumina Novaseq 6000 platform in a 2 × 150 bp paired-end configuration. GENEWIZ Biotechnology Co. LTD (Azenta Life Sciences, Shinagawa, Tokyo, Japan) carried out library preparation and sequencing.

The quality of raw sequencing data was first assessed with FastQC v.0.12.0, which allowed for the setting of the most appropriate trimming parameters for Trimmomatic v.0.40 [24] to remove sequencing adapters, low-quality bases, and failed reads. High-quality trimmed reads were *de novo* assembled using Trinity v.3 [25] with default parameters. The transcriptome assembly quality was assessed with BUSCO v5.7.1 [26] based on the set of conserved orthologous genes of the Metazoa lineage according to OrthoDB v.10 [27]. Nearly perfect matches with the partial amino acid sequence obtained through the Edman degradation were initially searched by selecting hits with tBLASTn matches scoring an e-value lower than 0.05 [28]. Matching nucleotide sequences were subjected to virtual translation to protein with the Expasy translate tool [29]. The full-length cDNA and protein sequences were deposited to GenBank, with the accession IDs PQ439878 and XHV10860.1.

2.5. 3-D structure model of HOL-30

The HOL-30 prediction models were generated as previously reported [4] using ColabFold [30], a Google Colab-based implementation of AlphaFold3 [31]. The output models were compared with known galectin structures, and the figures were visualized using ChimeraX [32].

2.6. Structural comparison of the N-terminal and C-terminal domains

The sequence alignment was performed using BLAST. The full-length structure of HOL-30 was predicted using AlphaFold3 [31]. The structural superposition of the N-terminal and C-terminal domains was conducted and visualized in PyMOL (ver. 1.8 2015, https://www.pymol.org/) .

2.7. Glycan-binding profiling of HOL-30

Glycan array analysis was performed by a system of Glycotechnica Co., Ltd. (Yokohama, Japan), as previously reported [6]. The lectin was fluorescence-labeled (λex/em 560/580 nm) using Cy3 labeling kit-NH_2 (Cytiva, Tokyo, Japan) per the manufacturer's instructions. A total of 28 glycans were immobilized on wells of a microarray. Fluorescence-labeled lectins at concentrations ranging from 0 to 100 μg/mL were incubated overnight at 4°C in the dark. The glycan-binding specificities of the lectin were detected by a GlycoLyte2200 Model evanescent fluorescence scanner (Glycotechnica Co., Ltd., Yokohama, Japan) with a modified version of a previously reported protocol [33,34].

2.8. Glycan docking simulation

The structure file of HOL-30 was modeled using AlphaFold3. The glycan ligand evaluated for binding with HOL-30 in section 2.7 was retrieved from the PubChem database in its 3D structure format. Docking simulations were performed using SwissDock [35], utilizing the AutoDock Vina scoring function [36]. The search space concentrated on a region associated with a known binding site identified for galectins. The ligand with the strongest binding affinity was chosen and presented as a representative result among the predicted binding poses.

2.9. Binding, internalization, and cell static activities of Porifera galectins on HeLa cells

The FITC-labeling kit labeled HOL-30 and hRTL as per the manufacturer's instructions. Human cervical cancer HeLa cells were chosen as the target cells to compare the lectin activities because the cells express both LacNAc and TF-antigen [37,38]. Cells cultured and maintained in RPMI 1640 supplemented with heat-inactivated FBS (10 %, v/v), penicillin (100 IU/mL), and streptomycin (100 μg/mL) at 37°C in 95 % air/ 5 % CO_2 atmosphere. Cells were washed 3 × with PBS, incubated two h with 10 μg/mL FITC-labeled HOL-30 and hRTL, nuclei stained by DAPI, and cells fixed with 4 % paraformaldehyde and observed by fluorescence microscopy ($\lambda_{ex/em}$=495/520 nm for FITC; 364/454 nm for DAPI) [36].

Cancer cells were maintained in RPMI 1640 supplemented with heat-inactivated FBS 10 % (v/v), penicillin (100 IU/mL), and streptomycin (100 μg/mL) at 37 °C. Cytotoxic effects and cell growth following treatment with HOL-30 at concentrations ranging from 0 to 100 μg/mL were determined using Cell Counting Kit-8 containing WST-8 [39]. Cells (2 × 104, in 90 μL solution) were seeded into 96-well flat-bottom plates and treated with ten μL lectin for 24 h at 37 °C. To assay the effect on cell growth, each well was added with ten μL WST-8 solution and incubated for 4 h at 37 °C. Cell survival rate was determined by measuring Abs 450 (reference: Abs 600) with an iMark microplate reader.

2.10. Generation of antiserum against HOL-30 and Localization of HOL-30 in sponge tissues

Antiserum against HOL-30 was raised according to a previously described method [40] in rabbit serum by Sigma-Aldrich Japan (Merck, Darmstadt, Germany). Antigen (500 μg synthesized peptide 127-ISENNAIHPTVKLG-140 in HOL-30) was injected thrice for every 20 days, and antiserum was collected using saturated NH_3SO_4. Crude sponge extract and purified HOL-30 separated by SDS-PAGE were electroblotted onto the PVDF membrane [41]. Colored standard marker protein was used as AE-1450 EzStandard PrestainBlue by ATTO (Tokyo, Japan). Blotted membrane was masked with TBS containing 1 % (w/v) BSA, soaked with 0.2 % Triton X-100 at room temperature, applied with anti-HOL-30 rabbit serum (1:1000 dilution) (primary antibody) and HRP-conjugated goat anti-rabbit IgG (secondary antibody) for 1 hour each, and colored with EzWestBlue as per the manufacturer's instructions.

The tissue localization of the lectin was observed using the same procedure [41]. Sponge tissues were excised, fixed in 4 % paraformaldehyde with 0.1 % glutaraldehyde in 0.1 M cacodylate buffer (pH 7.4) for two hours at four°C, dehydrated by ethanol dilution series, and embedded in Pathoprep-568. Sections were cut by microtome, mounted on poly-L-lysine-coated slides, deparaffinized by immersion in xylene, dehydrated ethanol, and ethanol dilution series, blocked overnight with 1 % (w/v) BSA containing TBS, applied with anti-HOL-30 antiserum (diluted 1:500 with TBS) and FITC-labeled anti-rabbit goat IgG for one h, and observed by fluorescence microscopy ($\lambda_{ex/em}$=495/520 nm). To show the outline of cells in the tissues, Nile Red solution was prepared with a concentration of 5 μg/mL in acetone, stained the slide for 30 min, observing the tissues by fluorescence microscopy ($\lambda_{ex/em}$=553/637 nm).

2.11. Statistical analysis

Experiments were performed in triplicate, and results were presented as mean ± standard error (SE). Data were subjected to a one-way analysis of variance (ANOVA) followed by Dunnett's test using the SPSS Statistics software package, v. 10 (www.ibm.com/products/spss-statistics, accessed on 5th Oct. 2024). Differences with $p < 0.05$ were considered significant.

3. Results

3.1. Overall RNA sequencing of H. okadai

Overall, using sponges *Halichondria okadai* collected at Sagami-Bay,

Japan (Suppl. Fig. S1A and B), RNA sequencing carried out on an Illumina platform, led to the generation of about 50 million high-quality raw paired-end reads, which were deposited in a public repository (NCBI BioProject: PRJNA1141218) and assembled to 147,581 unigenes. Both the high quality of the reads and the completeness of the transcriptome assembly (BUSCO scores indicated the presence of 93.8 % complete, 2.0 % fragmented, and 4.2 % missing conserved metazoan single copy orthologs) supported the reliability of this resource as a database for the identification of full-length protein sequences based on the identification of matching peptide fragments in this species (Suppl. Fig. S1C).

3.2. Characterization of the primary structure of HOL-30

A tBLASTn search allowed the identification of the complete protein sequence of a candidate HOL-30 sequence (Suppl. Fig. S2A), confirming

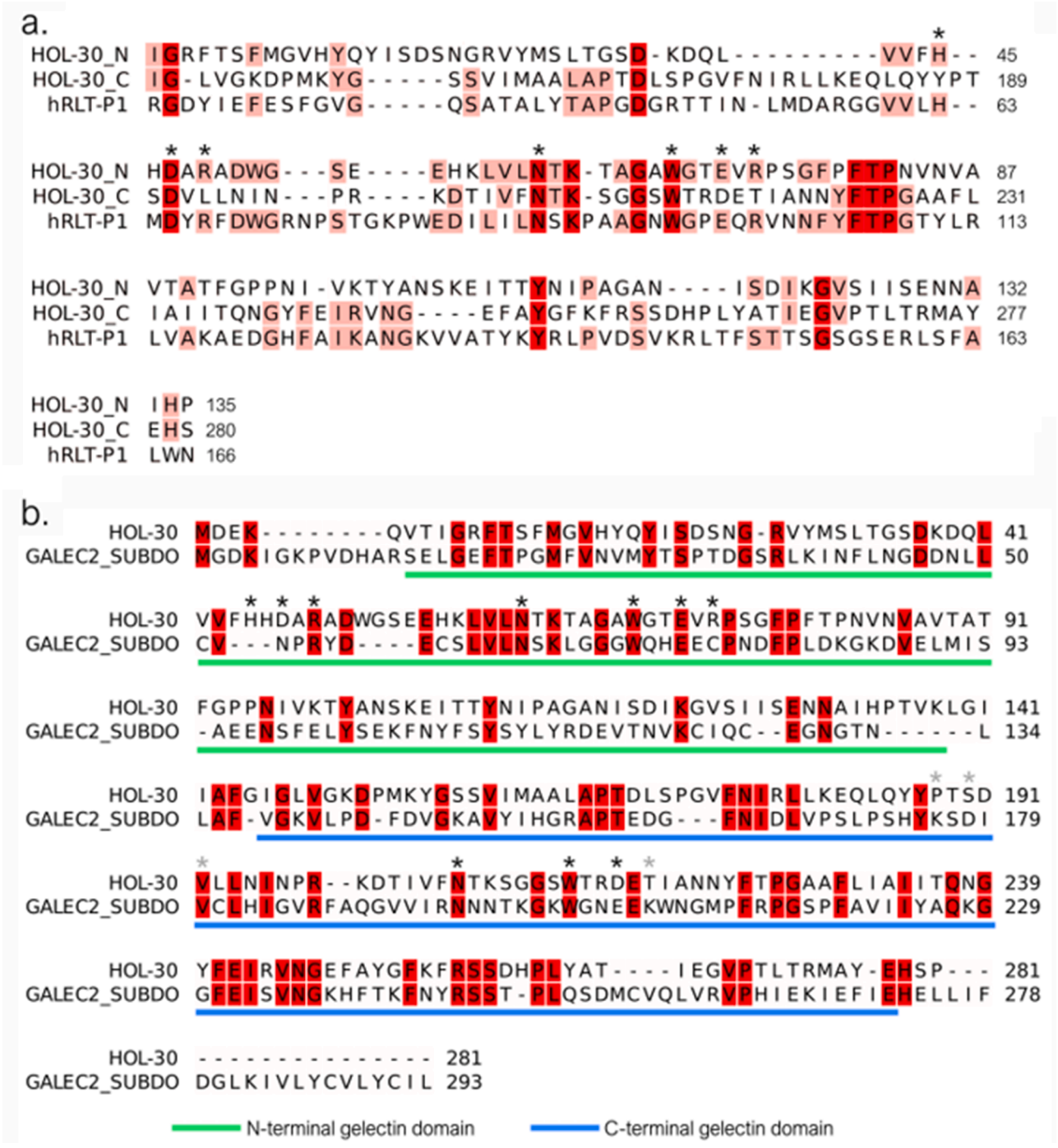

Fig. 1. Primary structure of HOL-30. **a**: multiple sequence alignment of HOL-30 N-terminal (HOL-30 N) and C-terminal (HOL-30 C) carbohydrate recognition domains and the single CRD of the *C. australiensis* proto-type galectin hRTL. The seven consensus amino acids of the galectin family are indicated as black asterisks. Highly conserved amino acids, shared by three or two CRDs, are highlighted in red and pink, respectively. **b**: primary amino acid sequence alignment between the two tandem-repeat type sponge galectins HOL-30 (*H. okadai*) and galectin_2 (*Suberites domuncula*) (GenBank: CAJ43112.1). Conserved amino acids are highlighted in red. The seven consensus amino acids of the galectin family are indicated as asterisks and colored depending on their conservation (black) or divergence (grey) with respect to the galectin consensus. The N-terminal and C-terminal CRDs are underlined with green and blue lines, respectively.

the matching with the lysyl-endopeptidase digested peptide sequences (Suppl. Fig. S2B, K1 to K6) determined by the Edman degradation [1]. Although several other expressed sequences in this species carried one or more galectin domains, only a single sequence displayed high primary sequence identity (i.e., 70 % at the amino acid level) with HOL-30. However, the corresponding assembled contig was incomplete at the 5'end and displayed a low coverage, which prevented the recovery of the complete amino acid sequence. Overall, these observations are consistent with the presence of a HOL-30 paralog in *H. okadai*, even though the biological relevance of this gene remains unclear in light of its low expression levels. This finding marked the first significant difference between HOL-30 and the *C. australiensis* hRTL, which was found to have five closely related expressed paralogous genes. Another striking difference was represented by the signal peptide sequence, which was present in hRTL but missing in HOL-30. In addition, Edman degradation analysis of HOL-30 revealed that the N-terminal amino acid was blocked with a chemical group [1], in contrast to hRTL, which had a free terminus. However, these observations are consistent with that most galectins lack a signal peptide targeted for secretion through a non-canonical pathway [42], thereby being N-terminally modified. The HOL-30 polypeptide consisted of 281 amino acids, and the molecular mass of the lectin was well-matched with SDS-PAGE determination (30 kDa). Unlike hRTL, which only displayed a single CRD, HOL-30 was a tandem-repeat type galectin consisting of two CRDs (Fig. 1a). The BLAST search showed that the primary sequence of HOL-30 displayed a moderate level of sequence identity with *Suberites domuncula* galectin-2, another tandem-repeat type of galectin previously described in another related species, belonging to the same order (Suberitida), but to a different family (Suberitidae) (Fig. 1b). The primary sequence of HOL-30 and *S. domuncula* Gal-2 shared ca. 28 % identical, while also considering conservative substitutions. In both sponge galectins, the linker peptide connecting the two CRDs was very short, being nearly absent (Fig. 1b red squares). Seven consensus amino acids used for glycan binding in the galectin CRD (Fig. 1 black asterisks) were also moderately conserved in each domain and each Porifera lectin (Fig. 1, red squares). There were no Cys residues in the HOL-30 polypeptide, though *S. domuncula* Gal-2 had 8 Cys residues in the polypeptide consisting of 293 amino acids. At the C-terminal end (residues 276–293), *S. domuncula* Gal-2 had a hydrophobic tail. However, it was absent in HOL-30.

3.3. 3D structure model of HOL-30

The 3D structure model of the tandem repeat HOL-30 subunit was graphically represented with the ChimeraX software version 1.8 (Fig. 2B). Each domain at N- and C-terminus was connecting twisted (Fig 2A and C). Despite a very low primary sequence identity (13 %), the tertiary structures of the N- and C-terminal domains were very similar (Fig. 3).

HOL-30's tertiary structure was overall like the human galectin-1 and the *C. australiensis* galectin hRTL (Supple Fig. S3). However, when the structures were superimposed, HOL-30 did not display an accessory loop that was present in a sponge galectin hRTL.

3.4. Molecular mass and hemagglutination activities of HOL-30

Gel permeation chromatography revealed that HOL-30 was a single polypeptide corresponding to a 30 kDa band (Fig. 4A, inserted an SDS-PAGE picture). In solution, however, HOL-30 exhibited a molecular mass of approximately 60 kDa (Fig. 4A), indicating a dimeric association of two galectin polypeptides, each containing a tandemly repeated carbohydrate-recognition domain (CRD). The protein concentration ratio to hemagglutination activity of HOL-30 was directly proportional (Fig. 4B), suggesting that HOL-30 binds stoichiometrically to glycans and cells without forming supramolecular complexes. This finding was used to determine the optimal concentration of HOL-30 for the glycan-binding property analyses described below.

3.5. The prediction of the dimeric structures

AlphaFold3 gave a high-confidence prediction for the monomeric structure with a pTM score of 0.84, which means the structure is well folded. However, the predicted scores were much lower for the dimeric form: ipTM = 0.27 and pTM = 0.58. The pTM score checks how similar the overall structure is to the proper structure, while ipTM looks at the accuracy of the interaction between subunits. Usually, if ipTM is below 0.6, the interface prediction is unreliable. So, it seems that AlphaFold3 could not predict the dimeric interaction correctly.

3.6. The glycan-binding properties

The glycan-binding profile of HOL-30 was analyzed by glycan array using 28 glycans (Suppl. Table S), highlighting the same pattern elucidated by frontal affinity chromatography [1]. In addition, critical new results were collected in comparison with the glycan-binding properties of hRTL.

Cy3 labeled HOL-30 (the titer was equivalent to 254 calculated by Fig. 4B) showed the highest binding to oligosaccharides of type-1 (Galβ1–-3GlcNAc) (**24**) and type-2 LacNAc (Galβ1–4GlcNAc) (**25**) (Fig. 5A). HOL-30 could bind to blood type H-glycans, especially those of type-3 (Fucα1–-2Galβ1–-3GalNAcα1-) (**11**), type-1 (Fucα1–2Galβ1–-3GlcNAcβ1-) (**9**), and type-2 (Fucα1–-2Galβ1–4GlcNAcβ1-) (**10**). However, the lectin did not recognize type-4 (Fucα1–-2Galβ1–-4GalNAcβ1-) (**12**) blood type H-glycan. HOL-30 also displayed a moderate binding to Thomsen–Friedenreich (TF)-disaccharide (Galβ1–-3GalNAc) (**20**), which is known as a cancer-specific glycan associated with mucin.

Another remarkable binding property of HOL-30 was the ability to recognize blood type B type-1 (Galα1–3[Fucα1–2]Galβ1–3GlcNAcα1-)

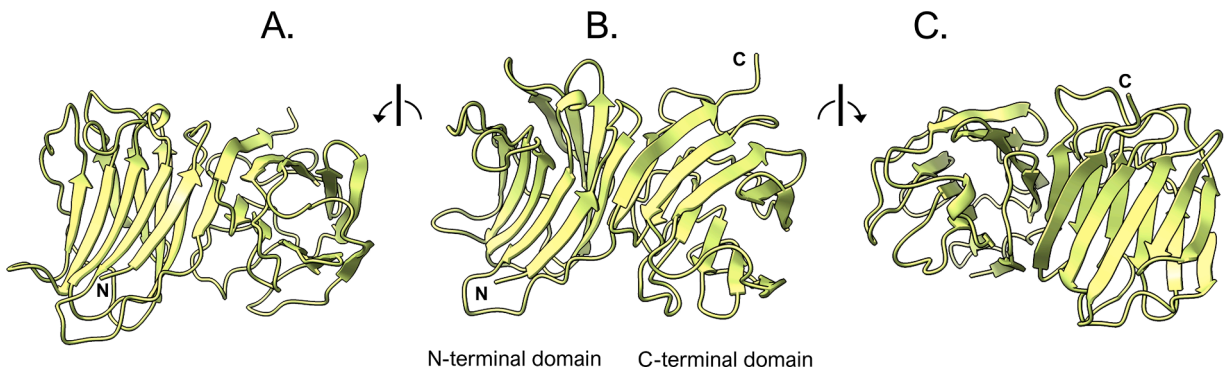

Fig. 2. 3D structure model of HOL-30. The views are from the side of the N-terminal domain (**A**), the whole figure (B), and the views are from the side of the C-terminal domain (**C**).

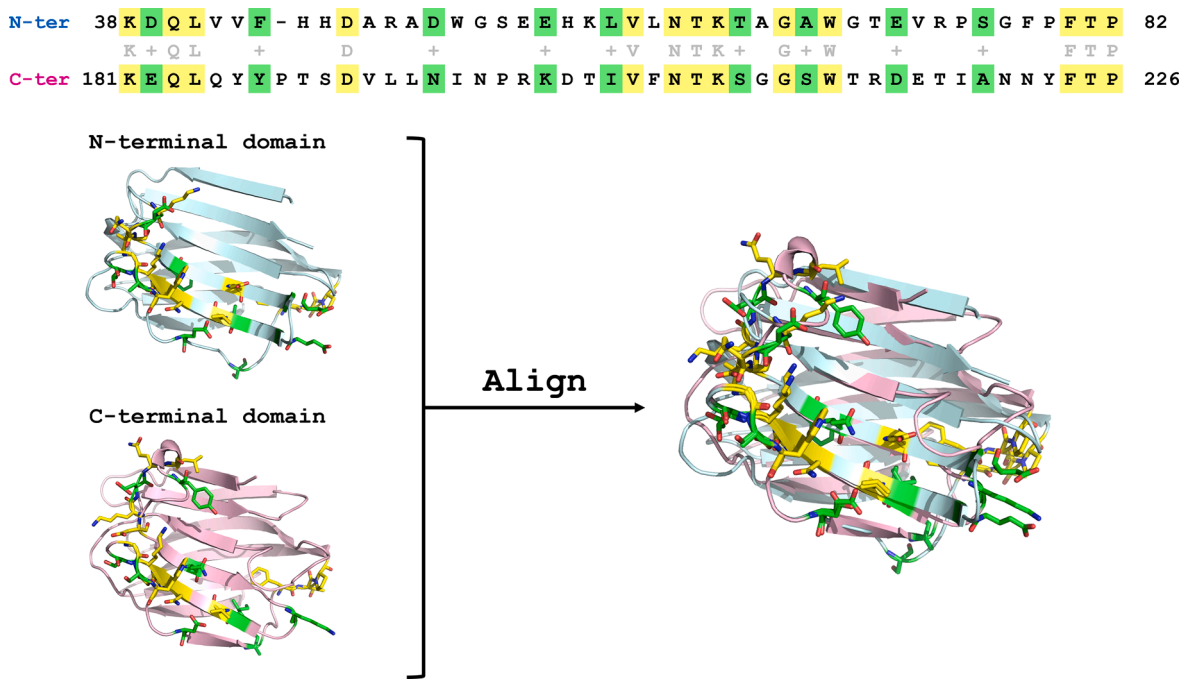

Fig. 3. Structural comparison of the N-terminal and C-terminal domains of HOL-30. The sequence alignment of the N-terminal and C-terminal domains highlights conserved and similar residues, with identical side chains shown in yellow and similar side chains in green. The structure model of HOL-30 was predicted using AlphaFold3, and the individual domain structures were subsequently superimposed to illustrate their similarity. The structural alignment resulted in a root-mean-square deviation (RMSD) of 2.6 Å, indicating a high degree of structural conservation despite sequence variations.

(**5**) and type-2 (Galα1–3[Fucα1–2]Galβ1–4GlcNAcα1-) (**6**). On the other hand, the lectin had very weak recognition of type-1 to type-4 (**1**–**4**) blood type A-glycans, type-3 (**7**), as well as type-4 (**8**) blood type B-glycans. Regarding type-1 and type-2 LacNAc, the binding of HOL-30 to Le^a, where Fuc is bound to the C4 position of GlcNAc (**13**), and Le^b, where Fuc is bound to the C3 position of Gal (**14**), was lost, identical to the binding loss observed for Le^x (**15**) and Le^y (**16**), which are composed of type-2 LacNAc. If compared to the glycan-binding pattern of hRTL, which specifically recognized type-1 and type-3 glycans [4], the glycan-binding properties of the two Porifera galectins were remarkably different (Fig. 5A vs B), In summary, HOL-30 preferentially recognized type-1, type-2 LacNAc glycans, and type-3 blood type H-glycan, in addition to type-1 and type-2 blood type B glycans.

3.7. Binding, incorporation, and cytotoxic activities of HOL-30 on HeLa cells

FITC-labeled HOL-30 bound to the surface of HeLa cells expressing both LacNAc and TF-antigen [25,26], being subsequently internalized (Fig. 6A). However, HOL-30 did not influence the cell proliferation of HeLa cells (Fig. 6B).

3.8. Localization of HOL-30 in sponge tissues

Anti-HOL-30 antiserum raised in rabbits was used to identify the lectin by western blotting analysis (Suppl. Fig. S5). A band with a molecular mass of 30,000 was detected in the crude extract of *H. okadai* by adding HRP-conjugated goat anti-rabbit IgG (Suppl. Fig. S5, columns 1–3). The position of the band was consistent with that of purified HOL-30 (Suppl. Fig. S5, columns 4 and 5). This antiserum allowed the detection of the localization of HOL-30 localized with a mosaic pattern in the parenchyma cells (oranges are cells in the sponge tissue stained by Nile Red) within sponge tissues (Fig. 7A). Further magnification revealed that the distribution of HOL-30 corresponded to the around spicules located in the parenchyma cells (Fig. 7A and B). HOL-30 was present in the cells and tissues covering the spicule fragments (Fig. 7C), which may be involved in the construction of the skeletal structures of the sponge. The location of HOL-30 seemed to be associated with these dense cells, suggesting that the spicules did not directly express HOL-30.

4. Discussion

Here, we report the *de novo* assembly of a highly complete transcriptome from *Halichondria okadai*, a well-known species due to its ability to bio-accumulate algal toxins, such as okadaic acid, in its tissues. We determined the complete primary structure of the tandem repeat-type galectin HOL-30 (Fig. 1, Suppl. Fig. S2), whose sequence analysis provided novel insights into the evolution of this lectin family in an early-branching metazoan phylum, as well as into the carbohydrate-binding properties of this lectin family.

From a comparative perspective, almost all sponge galectins discovered to date were prototypes (i.e. included a single CRD) [4–9, 11], except for a tandem repeat-type galectin previously described in *S. domuncula* [10]. The analysis of the newly generated transcriptome revealed the presence of multiple prototype galectins in *H. okadai* (data not shown), confirming the general notion that this galectin sub-type is the most widespread in sponges. It is generally believed that the tandem-repeat type galectins, which are found in several different animal phyla, evolved from the duplication of the CRD-encoding exon of an ancestral prototype gene. The discovery of HOL-30 confirms that this evolutionary process has also occurred in Porifera, even though it cannot clarify whether this CRD duplication event happened ancestrally, or in an independent manner in different phyla. However, no multi-tandem galectin, present in mussels [42] as well as in other bilateral symmetrical animals, was found in *H. okadai*. This is consistent with the notion that galectins underwent further diversification during animal evolution, in parallel with the occurrence of whole genome duplication events, the acquisition of bilateral symmetry, and the development of advanced physiological functions, including a more complex immune system [15].

Porifera offer an invaluable resource for investigating the reasons underlying the loss of the signal peptide sequence, that characterizes the

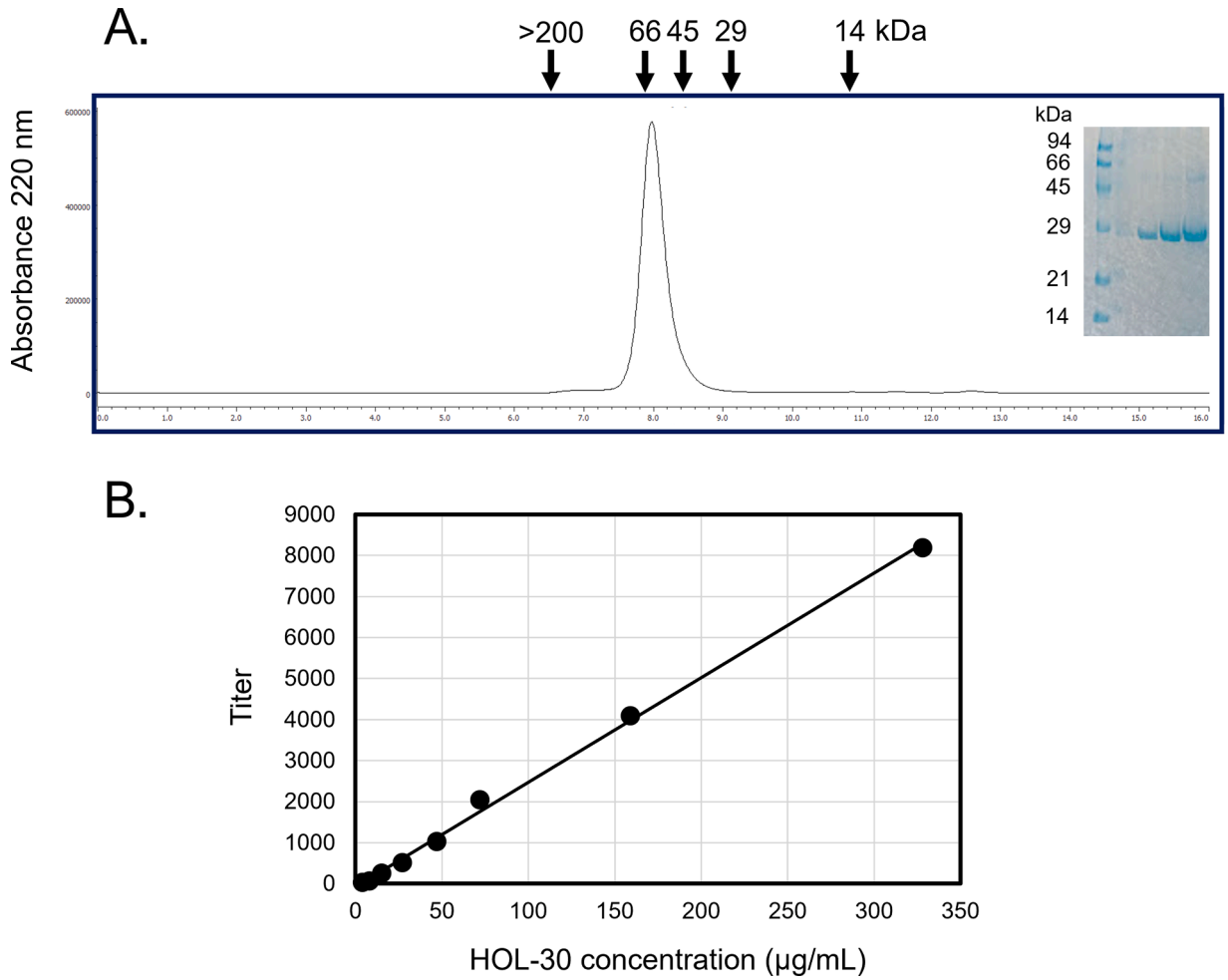

Fig. 4. Elution pattern of Gel permeation chromatography (GPC) and lectin scale of HOL-30. **A**: GPC pattern of HOL-30. Molecular markers are blue dextran (200 kDa), bovine serum albumin (66 kDa), ovalbumin (44 kDa), carbonic anhydrase (29 kDa), and lysozyme (14 kDa). Inserted: SDS-PAGE pattern of HOL-30 indicating 30 kDa in reducing conditions. **B**: lectin scale of HOL-30. The Y-axis indicates the hemagglutination titer measured at each protein concentration. The detailed hemagglutinating assay is cited in Suppl. Fig S4.

overwhelming majority of animal galectins, shedding light on the evolutionary diversification of these proteins across metazoan phylogeny. Could the evolutionary transition from the ancestral prototype galectin architecture to a tandem-type galectin organization explain the loss of signal peptides in sponges? Do sponges utilize both an unconventional lysosome-mediated secretion system, characteristic of galectins lacking a signal peptide, and a Golgi-mediated pathway for galectins with signal peptides, or have these systems converged to secrete galectins exclusively via the lysosome [43]? Various alternative interpretations are possible. Further comparative transcriptomic and genomic analyses of taxonomic groups relevant for investigating the ancestral origins of metazoan galectins might provide key insights into the mechanisms underlying the secretion of these carbohydrate-binding molecules.

The two CRDs of HOL-30 shared low primary sequence identity, standing at about 13 % (Fig. 3), a typical feature of vertebrate tandem repeat-type galectins. This observation suggests that acquiring a second CRD by HOL-30 galectins was not a mere domain duplication but involved the divergent evolution between the two CRDs, with possible important functional implications. The molecular mass of the lectin was determined to be 60kDa by GPC (Fig 4). Experimental data show that this protein naturally exists as a dimer in solution. However, AlphaFold3 could not predict this dimeric arrangement with high confidence. This difference may be because AlphaFold3 has difficulty predicting specific interactions between subunits or there are not enough similar structures in its training data. Because the ipTM score is very low, this computational prediction is unreliable and depends on experimental evidence instead. The glycan-binding properties of HOL-30 against types-1 and type-2 LacNAc, in addition to type-1 and type-2 blood type-B glycans (Fig. 5). This characters that have an affinity for both LacNAc and blood group glycans was likely to the tandem repeat-type galectin -4, -8, and -9 in mammals [44,45]. It may indicate that these glycan-binding properties were derived from poriferan tandem repeat type galectin, suggesting to be HOL-30 an ancestral form of vertebrate's tandem repeat type galectin. Docking simulations of each domain and glycan were performed to determine whether the N-terminal domain or the C-terminal domain has affinity for each glycan. However, AlphaFold3 predicted each glycan showed similar binding affinity to each domain (Suppl Fig. S6). These issues might be better measured physicochemically in future studies by individually expressing each CRD in bacteria and comparing their glycan-binding properties.The different glycan-binding features displayed by sponge lectins will affect the development of lectin-derived drugs. In any case, HOL-30 did not appear to have significant cytotoxicity compared to *C. australiensis* hRTL. This observation suggests that, regardless of the molecular mass of the non-covalently bound lectin complexes in solution (i.e. although both have a MW of 60kDa, HOL-30 consists of two 30kDa tandem-repeat-type (having 2 CRDs) subunits (Fig. 3 top). In contrast, hRTL consists of four 15kDa proto-type (having 1 CRD) subunits [6]), and the number of CRDs (both the HOL-30 and hRTL complexes have four CRDs each), each sponge

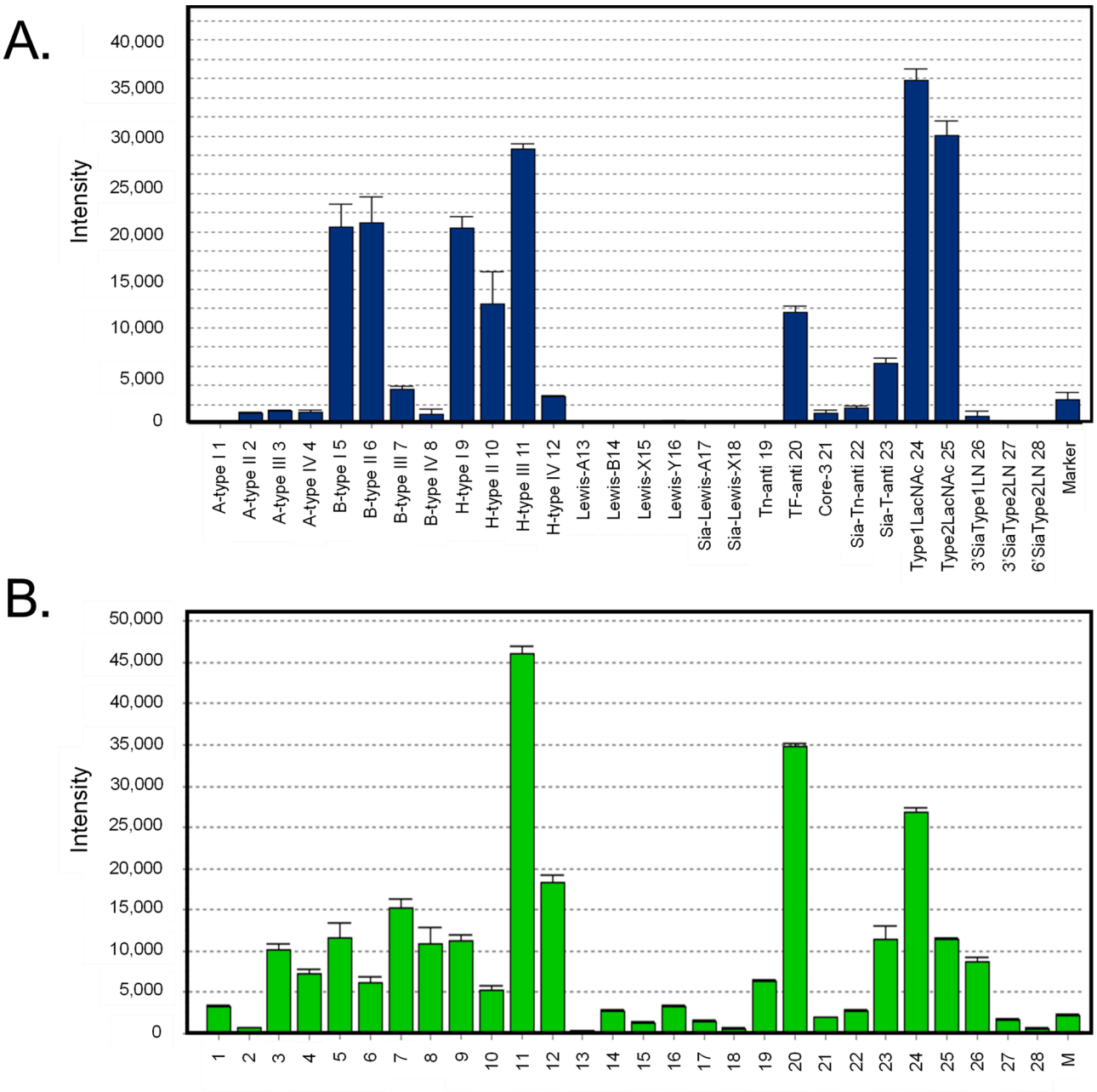

Fig. 5. Glycan-binding profile of HOL-30. **A**: Cy3-labeled HOL-30 was subjected to glycan array analysis combining a glycan-conjugated array with 28 immobilized glycan structures and a surface plasmon resonance scanning detector (the numbering in the X-axis is the same as in Suppl. Table S). The evanescent-field fluorescence occurring by the binding between Cy3-HOL-30 and the glycans is represented as a net intensity (Y-axis of the graph). **B**: A comparative profile of hRTL (referred from the previous data [6]).

galectin had widely different effects on cell regulation. This suggests that in addition to the molecular structure, the glycan-binding properties of these sponge galectins may significantly affect their ability to interact with cells and regulate their fate (Fig. 4A vs B). In any case, HOL-30 could serve as a valuable model lectin for investigating the role of glycans in cellular regulation. Administering HOL-30 to cells without inducing cytotoxicity would allow the identification of transcriptionally-regulated genes, providing insights into glycan function.

The distributions of HOL-30 in the tissue surrounding the spicules are consistent with the previous findings collected about another sponge tandem-repeat-type galectin, i.e. the *S. domuncula* galectin-2, which is involved in spicule morphogenesis by binding to spicule-forming proteins (silicatein) and collagens [10,46]. Since non-glycosylated ligands have also been previously reported for vertebrate galectins [47–49], it would not be particularly surprising to observe that these interactions are independent from the recognition of glycans. By examining the interactions between marine invertebrates, which have a minimal amount of galactoside sugars, and their living environment, we may uncover new interaction partners for galectins, revealing an original and still unknown role of galectins. The information provided by immunohistochemical studies aimed at clarifying the distinct localization of various lectins within sponge tissues will most likely offer insights into their physiological roles and may reveal valuable galectins for potential applications in drug discovery

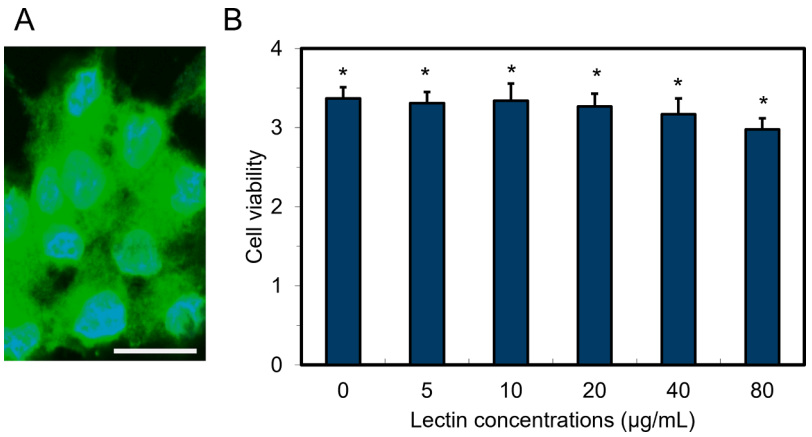

Fig. 6. Binding, internalization, and cell growth regulative activity of sponge galectins towards human cervical cancer cells. HeLa cells were treated with FITC-labeled HOL-30 (10 μg/mL) for two h at 37 °C. **A:** HOL-30. Nuclei were visualized by DAPI staining. Scale bar: 25 μm (white bar). **B:** HeLa cells were treated with HOL-30 at various concentrations (0–80 μg/mL) for 24 h, and cell viability was determined by WST-8 assay. The data shown are the mean ± SE (n = 3. *P* value (*$P < 0.05$).

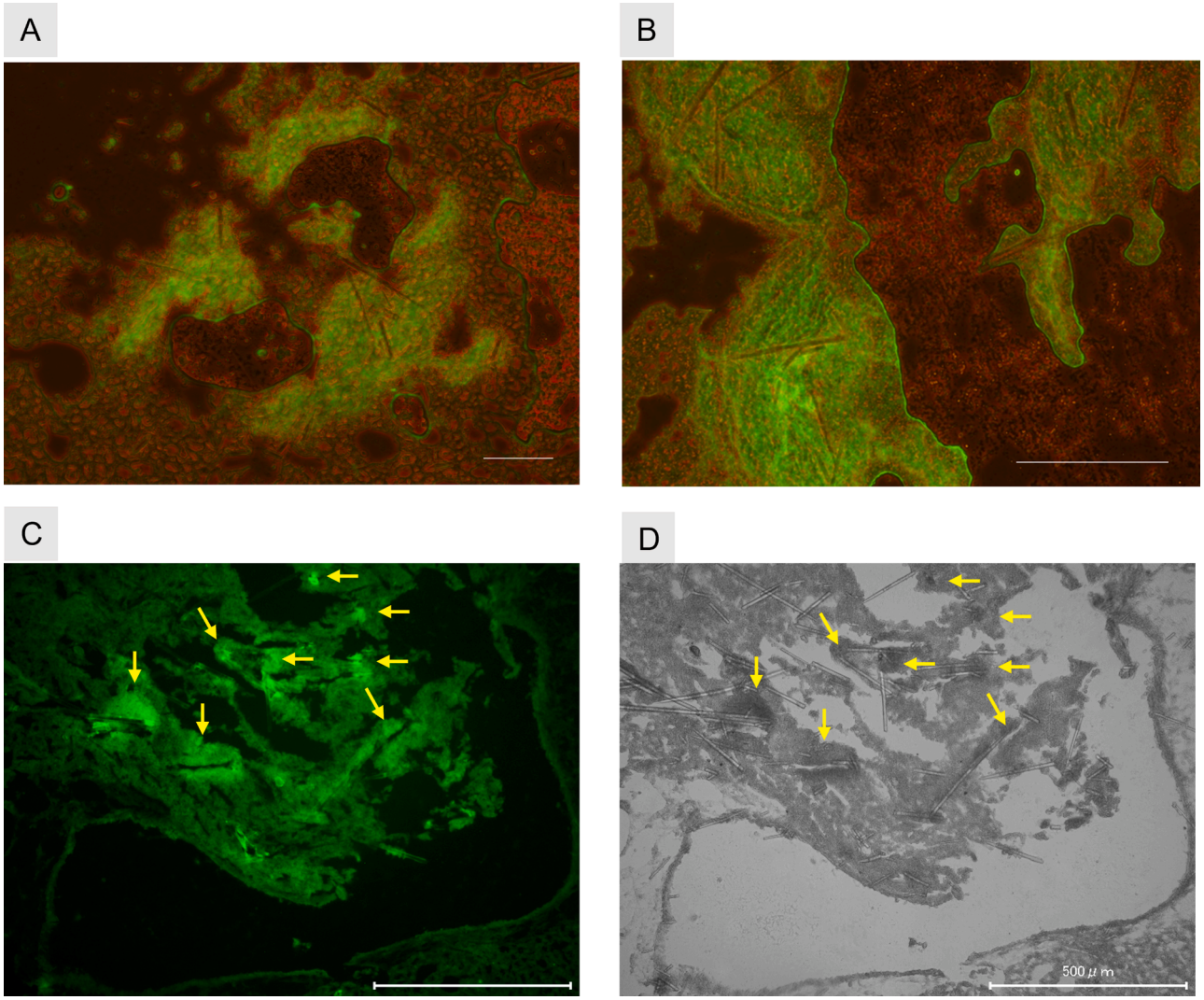

Fig. 7. Localization of HOL-30 in sponge tissue. Paraffin-embedded serial sections were immune-histochemical stained with antiserum against HOL-30 (A-C), followed by FITC-conjugated anti-rabbit IgG goat secondary antibody. They were observed by fluorescence microscopy (A-C: λex/em= 490/520 nm). The Nile Red staining (A and B: λex/em= 553/637 nm): double staining with anti-HOL-30 anti-serum. D is the phase-contrast microscopy view of the sponge tissue section. Yellow arrows indicate the presence of HOL-30 (C), and they were also superimposed in D. Scale bars (white): 500 μm.

5. Conclusion

This is the second reported example of a tandem repeat-type galectin in sponges. The slightly smaller size of this molecule (281 amino acids) compared with typical tandem repeat-type galectins from vertebrates was due to the near complete lack of the linker region between the two CRD. Moreover, unlike prototype sponge galectins, HOL-30 did not have a signal peptide region for secretion. This observation suggests that this ancestral feature might have been independently lost in tandem repeat-type galectins in different evolutionary lineages. The ability to bind blood group glycans, displayed by vertebrate tandem repeat-type galectins in vertebrates, was already present in Porifera, thereby suggesting a very ancient origin for this property. HOL-30 did not display any significant effect on growth-regulation effect on cultured cells, even though these expressed recognizable ligands, and the lectin was internalized upon binding. In early-branching metazoans, such as sponges, a relatively small number of molecular players are likely used to carry out multifunctional roles. Identifying the localization of different lectins within tissues through immunohistochemical analysis will offer insights into their physiological roles and could uncover valuable galectins for drug discovery applications.

CRediT authorship contribution statement

Mayuka Ohkawa: Writing – original draft, Visualization, Methodology, Investigation, Formal analysis, Data curation. **Kenichi Kamata:** Validation, Supervision, Software, Methodology, Investigation, Data curation. **Sarkar M.A. Kawsar:** Writing – review & editing, Supervision, Project administration, Conceptualization. **Marco Gerdol:** Writing – review & editing, Visualization, Supervision, Software, Investigation, Funding acquisition, Data curation. **Yuki Fujii:** Writing – review & editing, Resources, Project administration, Investigation, Funding acquisition, Formal analysis, Data curation, Conceptualization. **Yasuhiro Ozeki:** Writing – review & editing, Writing – original draft, Visualization, Supervision, Project administration, Investigation, Funding acquisition, Formal analysis, Data curation, Conceptualization.

Declaration of competing interest

The authors declare that they have no known competing financial interests or personal relationships that could have appeared to influence the work reported in this paper.

Acknowledgments

This work was supported by the Assisted Joint Research Program (Exploration type) FY2024 E-26 of the J-GlycoNet/iGCORE cooperative network, accredited by the Ministry of Education, Culture, Sports, Science and Technology, MEXT, Japan, as a Joint Usage/Research Center. Mayuka Ohkawa, Kenichi Kamata, Yuki Fujii, and Yasuhiro Ozeki are supported by a research grant (23K06190, 24KJ1875, 24K08716) from Japan Society for the Promotion of Science (JSPS). Marco Gerdol is supported by the Interconnected Nord-Est Innovation Ecosystem (iNEST) and received funding from the European Union Next-GenerationEU (PIANO NAZIONALE DI RIPRESA E RESILIENZA (PNRR)—MISSIONE 4 COMPONENTE 2, INVESTIMENTO 1.5—D.D. 1058 23/06/2022, ECS00000043. Yasuhiro Ozeki is supported by the Yokohama Trial Grant for Research and Development YT2024–1050 from the City of Yokohama.

Supplementary materials

Supplementary material associated with this article can be found, in the online version, at doi:10.1016/j.bbadva.2025.100153.

Data availability

Data will be made available on request.

References

[1] S.M. Kawsar, Y. Fujii, R. Matsumoto, T. Ichikawa, H. Tateno, J. Hirabayashi, H. Yasumitsu, C. Dogasaki, M. Hosono, K. Nitta, J. Hamako, T. Matsui, Y. Ozeki, Isolation, purification, characterization and glycan-binding profile of a D-galactoside specific lectin from the marine sponge, *Halichondria okadai*, Comp. Biochem. Physiol. B Biochem. Mol. Biol. 150 (2008) 349–357.

[2] Chapter 36 R.D. Cummings, F.T. Liu, G.A. Rabinovich, S.R. Stowell, G.R. Vasta, Galectins, editors, in: A. Varki, R.D. Cummings, J.D. Esko, P. Stanley, G.W. Hart, M. Aebi, D. Mohnen, T. Kinoshita, N.H. Packer, J.H. Prestegard, R.L. Schnaar, P. H. Seeberger (Eds.), Essentials of Glycobiology, 4th ed., Cold Spring Harbor Laboratory Press, 2022, pp. 491–503.

[3] H. Leffler, S. Carlsson, M. Hedlund, Y. Qian, F. Poirier, Introduction to galectins, Glycoconj. J. 19 (2002) 433–440.

[4] J. Schütze, A. Krasko, M.R. Custodio, S.M. Efremova, I.M. Müller, W.E. Müller, Evolutionary relationships of Metazoa within the eukaryotes based on molecular data from Porifera, Proc. Biol. Sci. 266 (1999) 63–73.

[5] R.C.F. Torres, I.F.B. Júnior, V.R.P. Souza, J.A. Duarte, R.P Chaves, M.F.D. Costa Filho, E. Nascimento, E.A. Malveira, A.L. Andrade, U. Pinheiro, M.A. Vasconcelos, B.L. de Sousa, E.H. Teixeira, R.F. Carneiro, C.S. Nagano, A.H. Sampaio, Structural insights and antimicrobial synergy of a proto-galectin from the marine sponge *aiolochroia crassa*, Comp. Biochem. Physiol. B Biochem. Mol. Biol. 275 (2025) 111034.

[6] R. Hayashi, K. Kamata, M. Gerdol, Y. Fujii, T. Hayashi, Y. Onoda, N. Kobayashi, S. Furushima, R. Ishiwata, M. Ohkawa, N. Masuda, Y. Niimi, M. Yamada, D. Adachi, S.M.A. Kawsar, S. Rajia, I. Hasan, S. Padma, B.P. Chatterjee, Y. Ise, R. Chida, K. Hasehira, N. Miyanishi, T. Kawasaki, Y. Ogawa, H. Fujita, A. Pallavicini, Y. Ozeki, Novel galectins purified from the sponge *Chondrilla australiensis*: unique structural features and cytotoxic effects on colorectal cancer cells mediated by TF-antigen binding, Mar. Drugs 22 (2024) 400.

[7] J.A. Duarte, J.E. Oliveira Neto, R.C.F. Torres, A.R.O. Sousa, A.L. Andrade, R. P. Chaves, R. Carneiro, M.A. Vasconcelos, C.S. Teixeira, E.H. Teixeira, C.S. Nagano, A.H. Sampaio, Structural characterization of a galectin from the marine sponge *aplysina lactuca* (ALL) with synergistic effects when associated with antibiotics against bacteria, Biochimie 214 (2023) 165–175.

[8] A.R.O. Sousa, F.R.N. Andrade, R.P. Chaves, B.L. Sousa, D.B. Lima, R.O.D.S. Souza, C.G.L. da Silva, C.S. Teixeira, A.H. Sampaio, C.S. Nagano, R.F. Carneiro, Structural characterization of a galectin isolated from the marine sponge *Chondrilla caribensis* with leishmanicidal potential, Biochim. Biophys. Acta 1865 (2021) 129992.

[9] T. Ueda, Y. Nakamura, C.M. Smith, B.A. Copits, A. Inoue, T. Ojima, S. Matsunaga, G.T. Swanson, R. Sakai, Isolation of novel prototype galectins from the marine ball sponge Trimmomatic *Cinachyrella* sp. guided by their modulatory activity on mammalian glutamate-gated ion channels, Glycobiology 23 (2013) 412–425.

[10] H.C. Schröder, A. Boreiko, M. Korzhev, M.N. Tahir, W. Tremel, C. Eckert, H. Ushijima, I.M. Müller, W.E. Müller, Co-expression and functional interaction of silicatein with galectin: matrix-guided formation of siliceous spicules in the marine demosponge *Suberites domuncula*, J. Biol. Chem. 281 (2006) 12001–12009.

[11] K. Pfeifer, M. Haasemann, V. Gamulin, H. Bretting, F. Fahrenholz, W.E. Müller, S-type lectins occur also in invertebrates: high conservation of the carbohydrate recognition domain in the lectin genes from the marine sponge *Geodia cydonium*, Glycobiology 3 (1993) 179–184.

[12] D.M. Freymann, Y. Nakamura, P.J. Focia, R. Sakai, G.T. Swanson, Structure of a tetrameric galectin from *Cinachyrella* sp. (ball sponge), Acta Crystallogr. D. Biol. Crystallogr. 68 (2012) 1163–1174.

[13] C. Wagner-Hülsmann, N. Bachinski, B. Diehl-Seifert, B. Blumbach, R. Steffen, Z. Pancer, W.E. Müller, A galectin links the aggregation factor to cells in the sponge (*Geodia cydonium*) system, Glycobiology 6 (1996) 785–793.

[14] M. Srivastava, O. Simakov, J. Chapman, B. Fahey, M.E. Gauthier, T. Mitros, G. S. Richards, C. Conaco, M. Dacre, U. Hellsten, C. Larroux, N.H. Putnam, M. Stanke, M. Adamska, A. Darling, S.M. Degnan, T.H. Oakley, D.C. Plachetzki, Y. Zhai, M. Adamski, A. Calcino, S.F. Cummins, D.M. Goodstein, C. Harris, D.J. Jackson, S. P. Leys, S. Shu, B.J. Woodcroft, M. Vervoort, K.S. Kosik, G. Manning, B.M. Degnan, D.S. Rokhsar, The *Amphimedon queenslandica* genome and the evolution of animal complexity, Nature 7307 (2010) 720–726.

[15] J. Günther, S.P.A. Galuska, A brief history of galectin evolution, Front. Immunol. 14 (2023) 1147356.

[16] F.G. Hanisch, S.E. Baldus, T.A. Kümmel, Forssman disaccharide is the specific ligand of a galectin from the sponge *Geodia cydonium* but does not mediate its binding to nuclear protein np56, Glycobiology 6 (1996) 321–336.

[17] K. Martinez, J. Agirre, Y. Akune, K.F. Aoki-Kinoshita, C. Arighi, K.B. Axelsen, E. Bolton, E. Bordeleau, N.J. Edwards, E. Fadda, T. Feizi, C. Hayes, C.M. Ives, H. J. Joshi, K. Krishna Prasad, S. Kossida, F. Lisacek, Y. Liu, T. Lütteke, J. Ma, A. Malik, M. Martin, A.Y. Mehta, S. Neelamegham, K. Panneerselvam, R. Ranzinger, S. Ricard-Blum, G. Sanou, V. Shanker, P.D. Thomas, M. Tiemeyer, J. Urban, R. Vita, J. Vora, Y. Yamamoto, R. Mazumder, in: Functional implications of glycans and their curation: insights from the workshop held at the 16th Annual International Biocuration Conference in Padua, Italy, 2024. Database (Oxford) 2024baae073.

[18] N. de Haan, M. Pučić-Baković, M. Novokmet, D. Falck, G. Lageveen-Kammeijer, G. Razdorov, F. Vučković, I. Trbojević-Akmačić, O. Gornik, M. Hanić, M. Wuhrer,

G. Lauc, Developments and perspectives in high-throughput protein glycomics: enabling the analysis of thousands of samples, Glycobiology 32 (2022) 651–663.
[19] U.K. Laemmli, Cleavage of structural proteins during the assembly of the head of bacteriophage T4, Nature 227 (1970) 680–685.
[20] H. Yasumitsu, Y. Ozeki, S.M. Kawsar, T. Toda, R. Kanaly, CGP stain: an inexpensive, odorless, rapid, sensitive, and in principle in vitro methylation-free Coomassie Brilliant Blue stain, Anal. Biochem. 406 (2010) 86–88.
[21] P.K. Smith, R.I. Krohn, G.T. Hermanson, A.K. Mallia, F.T. Gartner, M. D. Provenzano, E.K. Fujimoto, N.M. Goeke, B.J. Olson, D.C. Klenk, Measurement of protein using bicinchoninic acid, Anal. Biochem. 150 (1985) 76–85.
[22] K.J. Wiechelman, R.D. Braun, J.D. Fitzpatrick, Investigation of the bicinchoninic acid protein assay: identification of the groups responsible for color formation, Anal. Biochem. 175 (1988) 231–237.
[23] J.P. Gourdine, G. Cioci, L. Miguet, C. Unverzagt, D.V. Silva, A. Varrot, C. Gautier, E.J. Smith-Ravin, A. Imberty, High affinity interaction between a bivalve C-type lectin and a biantennary complex-type *N*-glycan revealed by crystallography and microcalorimetry, J. Biol. Chem. 283 (2008) 30112–30120.
[24] A.M. Bolger, M. Lohse, B. Usadel, Trimmomatic: A flexible trimmer for Illumina sequence data, Bioinformatics. 30 (2014) 2114–2120.
[25] M.G. Grabherr, B.J. Haas, M. Yassour, J.Z. Levin, D.A. Thompson, I. Amit, X. Adiconis, L. Fan, R. Raychowdhury, Q. Zeng, Full-length transcriptome assembly from RNA-seq data without a reference genome, Nat. Biotechnol. 29 (2011) 644–652.
[26] AM. Manni, M.R. Berkeley, M. Seppey, F.A. Simão, E.M. Zdobnov, BUSCO Update: novel and streamlined workflows along with broader and deeper phylogenetic coverage for scoring of eukaryotic, prokaryotic, and viral genomes, Mol. Biol. Evol. 38 (2021) 4647–4654.
[27] D. Kuznetsov, F. Tegenfeldt, M. Manni, M. Seppey, M. Berkeley, E.V. Kriventseva, E.M. Zdobnov, OrthoDB v11: annotation of orthologs in the widest sampling of organismal diversity, Nucleic. Acids. Res. 51 (2023) 445–451.
[28] S.F. Altschul, W. Gish, W. Miller, E.W. Myers, D.J. Lipman, Basic local alignment search tool, J. Mol. Biol. 215 (1990) 403–410.
[29] E. Gasteiger, A. Gattiker, C. Hoogland, I. Ivanyi, R.D. Appel, A. Bairoch, ExPASy: the proteomics server for in-depth protein knowledge and analysis, Nucleic. Acids. Res. 31 (2003) 3784–3788.
[30] M. Mirdita, K. Schütze, Y. Moriwaki, L. Heo, S. Ovchinnikov, M. Steinegger, ColabFold: making protein folding accessible to all, Nat. Methods 19 (2022) 679–682.
[31] J. Abramson, J. Adler, J. Dunger, R. Evans, T. Green, A. Pritzel, Q. Ronneberger, L. Willmore, A.J. Ballard, J. Bambrick, S.W. Bodenstein, D.A. Evans, C.C. Hung, M. O'Neill, D. Reiman, K. Tunyasuvunakool, Z. Wu, A. Žemgulytė, E. Arvaniti, C. Beattie, O. Bertolli, A. Bridgland, A. Cherepanov, M. Congreve, A.I. Cowen-Rivers, A. Cowie, M. Figurnov, F.B. Fuchs, H. Gladman, R. Jain, Y.A. Khan, C.M. R. Low, K. Perlin, A. Potapenko, P. Savy, S. Singh, A. Stecula, A. Thillaisundaram, C. Tong, S. Yakneen, E.D. Zhong, M. Zielinski, A. Žídek, V. Bapst, P. Kohli, M. Jaderberg, D. Hassabis, J.M. Jumper, Accurate structure prediction of biomolecular interactions with AlphaFold 3, Nature 630 (2024) 493–500.
[32] T.D. Goddard, C.C. Huang, E.C. Meng, E.F. Pettersen, G.S. Couch, J.H. Morris, T. E. Ferrin, UCSF ChimeraX: meeting modern challenges in visualization and analysis, Protein Sci. 27 (2018) 14–25.
[33] A. Kuno, N. Uchiyama, S. Koseki-Kuno, Y. Ebe, S. Takashima, M. Yamada, J. Hirabayashi, Evanescent-field fluorescence assisted lectin microarray: A new strategy for glycan profiling, Nat. Methods 2 (2005) 851–856.
[34] J. Hirabayashi, M. Yamada, A. Kuno, H. Tateno, Lectin microarrays: concept, principle and applications, Chem. Soc. Rev. 42 (2013) 443–458.
[35] M. Bugnon, U.F. Röhrig, M. Goullieux, M.A.S. Perez, A. Daina, Michielin O, M. Zoete, SwissDock 2024: major enhancements for small-molecule docking with attracting cavities and AutoDock Vina, Nucleic. Acids. Res. 52 (2024) 324–332.
[36] J. Eberhardt, D. Santos-Martins, A.F. Tillack, S. Forli, AutoDock Vina 1.2.0: new docking methods, expanded force field, and Python bindings, J. Chem. Inf. Model. 61 (2021) 3891–3898.
[37] T. Kitagawa, Y. Tsuruhara, M. Hayashi, T. Endo, E.J. Stanbridge, A tumor-associated glycosylation change in the glucose transporter GLUT1 controlled by tumor suppressor function in human cell hybrids, J. Cell Sci. 108 (1995) 3735–3743.
[38] Y. Li, Y. Li, J. Xia, Q. Yang, Y. Chen, H. Sun, 3′-Sulfo-TF antigen determined by GAL3ST2/ST3GAL1 is essential for antitumor activity of fungal galectin AAL/AAGL, ACS. Omega 6 (2021) 17379–17390.
[39] H. Ukeda, D. Kawana, S. Maeda, M. Sawamura, Spectrophotometric assay for superoxide dismutase based on the reduction of highly water-soluble tetrazolium salts by xanthine-xanthine oxidase, Biosci. Biotechnol. Biochem. 63 (1999) 485–488.
[40] I. Hasan, Y. Ozeki, Histochemical localization of N-acetylhexosamine-binding lectin HOL-18 in *Halichondria okadai* (Japanese black sponge), and its antimicrobial and cytotoxic anticancer effects, Int. J. Biol. Macromol. 124 (2019) 819–827.
[41] A. Goldman, J.A. Ursitti, J. Mozdzanowski, D.W. Speicher, Electroblotting from polyacrylamide gels, Curr. Protoc. Protein Sci. 82 (2015) 1–16.
[42] M. Gerdol, P. Venier, An updated molecular basis for mussel immunity, Fish. Shellfish. Immunol. 46 (2015) 17–38.
[43] S.J. Popa, S.E. Stewart, K. Moreau, Unconventional secretion of annexins and galectins, Semin. Cell Dev. Biol. 83 (2018) 42–50.
[44] O.A. Vokhmyanina, E.M. Rapoport, S. André, V.V. Severov, I. Ryzhov, G. V. Pazynina, E. Korchagina, H.J. Gabius, N.V. Bovin, Comparative study of the glycan specificities of cell-bound human tandem-repeat-type galectin-4, -8 and -9, Glycobiology 22 (2012) 1207–1217.
[45] K. Slámová, J. Červený, Z. Mészáros, T. Friede, D. Vrbata, V. Křen, P. Bojarová, Oligosaccharide ligands of galectin-4 and its subunits: multivalency scores highly, Molecules. 28 (2023) 4039.
[46] C. Eckert, H.C. Schröder, D. Brandt, S. Perovic-Ottstadt, W.E. Müller, Histochemical and electron microscopic analysis of spiculogenesis in the demosponge *Suberites domuncula*, J. Histochem. Cytochem. 54 (2006) 1031–1040.
[47] G. Elad-Sfadia, R. Haklai, E. Balan, Y. Kloog, Galectin-3 augments K-ras activation and triggers a Ras signal that attenuates ERK but not phosphoinositide 3-kinase activity, J. Biol. Chem. 279 (2004) 34922–34930.
[48] T.L. Thurston, M.P. Wandel, N. von Muhlinen, A. Foeglein, F. Randow, Galectin 8 targets damaged vesicles for autophagy to defend cells against bacterial invasion, Nature 482 (2012) 414–418.
[49] S. Chauhan, S. Kumar, A. Jain, M. Ponpuak, M.H. Mudd, T. Kimura, S.W. Choi, R. Peters, M. Mandell, J.A. Bruun, T. Johansen, V. Deretic, TRIMs and galectins globally cooperate and TRIM16 and galectin-3 co-direct autophagy in endomembrane damage homeostasis, Dev. Cell 39 (2016) 13–27.